

A Study of the Effects of the External Environment and Driving Modes on Electric Automotive Air-Conditioning Load

Yew Khoy Chuah and Yu-Tsuen Chen

1 Introduction

According to the International Energy Agency (IEA) (2013) the oil consumption of OECD countries in the first quarter of 2013 amounts to 46 million barrels per day, a reduction of 200 thousand barrels with respect to the same period in 2012. However, there was an increase of 1.3 million barrels per day for non-OECD countries, up to about 44 million barrels per day.

The above figures clearly state the problem of our ever-increasing need for oil. Material needs in all aspects of comfortable modern life that are a consequence of economic growth will further aggravate our ever-growing need for energy. Inevitably the global warming problem resulting from the increasing atmospheric concentration of CO₂ is becoming worse each year.

Of all sectors of our lives, the internal combustion engine automobile is one of the largest sources of CO₂ emission. Hence electric-powered or hybrid-powered vehicles are seen to be a solution to reducing the need for oil. Conventional automobile air conditioning is powered by coupling to the engine. The air-conditioning system for hybrid- or electric-powered vehicles has to be electric powered. In addition, intelligent control adapted to driving modes is needed to reduce the power consumption and prolong the driving range. Therefore optimization of energy efficiency by control strategies is imperative. However, energy saving that does not affect driving thermal comfort has to be achieved.

Nakane et al. (2010) found that when all driving modes are considered, an air-conditioning system may reduce the driving range by one-half. Factors

Y.K. Chuah (✉) • Y.-T. Chen

Department of Energy and Refrigerating Air-Conditioning Engineering, National Taipei University of Technology, 1, Sec. 3, Zhongxiao E. Road, Taipei 10608, Taiwan
e-mail: yhtsai@ntut.edu.tw

considered in their research included the external environment, driving mode such as idling or moving, solar radiation angles, etc., that would greatly affect the cooling load. They also suggested that intelligent energy saving control would elevate energy management and greatly prolong the driving time without comprising thermal comfort.

Makino et al. (2003) suggested that a commercial compact scroll compressor can be used in electric vehicles. In comparison, it is smaller in size and has higher energy efficiency. Hosoz and Direk (2006) evaluated the use of a four-way valve so to provide heating in winter. They found that the heat exchanger has to be redesigned to achieve effective heating.

Brown (2009) compared the use of a new low GWP HFO refrigerant to the current R134a applied to automobiles. Although HFO refrigerant has thermal properties close to those of R134a, he suggested that more information is needed for further evaluation. Lee and Jung (2012) compared R1234yf to R134a under the same operating experimental conditions and found that R1234yf had a lower cooling capacity.

Alkan and Hosoz (2010) found that when the condenser fan of an automobile's air conditioner has variable speed control, variable speed compressor will perform better than that of a constant speed compressor.

2 Cooling Load Computation

Air-conditioning load is fundamental to the design and selection of equipment. A cooling computation model is proposed in this paper. In the proposed model, vehicle cooling load calculation is based on inputs of ambient air temperature, wind speed, solar radiation, driving mode, and passenger metabolism heat, among other things. The calculation also considers the vehicle's shell structure and materials, radiation angle at the glass, low-e glass application, occupancy, and outdoor air. Heat conduction, convection, and radiation are all considered in the model. Radiation transmitted through the large glass area with respect to the different incidence angles was considered in the model. The model allows for part of the glass having low emissivity coating as for most vehicles sold in Taiwan. For heat conduction through the body of the vehicle, an effective temperature was used instead of outdoor air temperature to account for solar radiation effects. A prediction of the external car body temperature was also made.

The total cooling load of an automobile can be calculated using Eq. (1), which is also shown schematically in Fig. 1.

$$Q_{\text{total}} = Q_{\text{solar}} + Q_{\text{cond}} + Q_{\text{fresh}} + Q_{\text{inside}} \quad (1)$$

Q_{total} : heat removed from inside an automobile (W)

Q_{solar} : Solar radiation through glass (W)

Q_{cond} : Heat conduction into automobile(W)

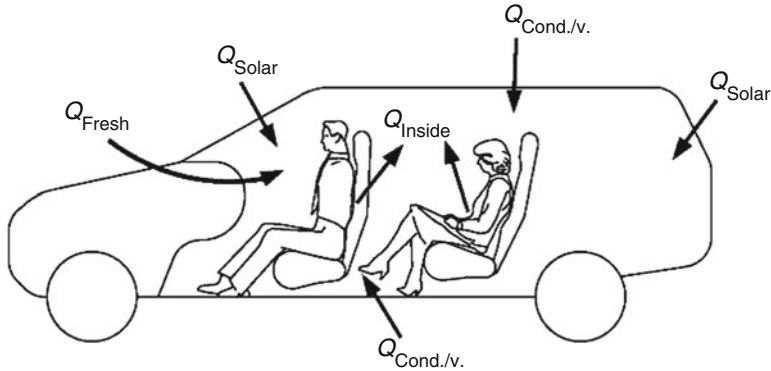


Fig. 1 Cooling load considered in the analysis

Q_{fresh} : Treating outdoor air to inside conditions (W)

Q_{inside} : Internal heat due to passengers and others (W)

2.1 External Convective Transfer Coefficient h_o

Heat convection between the external automobile surface and ambient air was considered in the analysis. In this study natural convection due to temperature difference was also considered. Heat transfer coefficients were calculated by referring to chapter 4 of the ASHRAE Handbook-Fundamentals (2009a).

2.2 Transmitted Solar Radiation Q_{Solar}

Automobiles with a large glass area transmitting solar radiation have a major source of air-conditioner load. The direct solar heat is affected by the transmittance, reflectivity, and absorptivity of the glass material or coating on it. Moreover, the glass thickness and solar incidence angle are also important factors to consider, as stated in chapter 14 of the ASHRAE Handbook-Fundamentals (2009b). The transmitted solar radiation can be calculated as shown in Eq. (2).

$$Q_{Solar} = \sum [T_b E_{t,b} + T_d (E_{t,d} + E_{t,r})] A_g \tag{2}$$

T_b : Solar direct transmittance, fraction

T_d : Solar diffuse transmittance, fraction

$E_{t,b}$: Solar direct intensity ($W.m^{-2}$)

$E_{t,d}$: Solar diffuse intensity ($W.m^{-2}$)

$E_{t,r}$: Surface reflectance ($\text{W}\cdot\text{m}^{-2}$)

A_g : Glass area (m^2)

There are some cases where the glass area has a coating to isolate some solar radiation. Normally the isolation effect can be as high as 65%. Therefore for a glass area with isolation coating Q_{solar} has to be revised, as in Eq. (3).

$$Q'_{\text{solar}} = Q_{\text{solar}} (1 - \text{isolation}) \quad (3)$$

2.3 Heat Conduction $Q_{\text{Cond.}}$

When the shell structure of an automobile is exposed to outside conditions, the external surface temperature is substantially higher than that of the internal surface. The external surface temperature is affected by solar radiation, outside air temperature, and driving speed. The glass area can be assumed to have a low thermal mass. However, for an opaque shell, heat conductivity has to be considered in the calculation. Moreover, the inside and outside convective heat resistance also has to be considered.

To simplify the computation the internal convective resistance is taken to be a constant value. The conduction calculation begins with the external surface temperature, therefore only internal convective resistance is considered. The calculation of heat conduction and the overall heat transfer coefficient U are calculated by Eqs. (4) and (5). In Eq. (5) ra is the resistance of the air gap in the automobile shell structure and t_{set} is the air-conditioning temperature set.

$$Q_{\text{cond}} = \sum UA(t_{\text{es}} - t_{\text{set}}) \quad (4)$$

$$U = \frac{1}{\sum d_j/k_j} + ra + 1/h_i \quad (5)$$

2.3.1 External Surface Temperature T_{es}

As shown in Fig. 2, the solar heat absorbed would partly be transmitted into the inside, but also partly reradiated or convected to the outside air. As can be seen in Eq. (6), heat conduction is balanced by three heat transfer mechanisms.

$$q''_{\text{conduction}} = q''_{\text{solar}} + q''_{\text{convection}} + q''_{\text{radiation}} \quad (6)$$

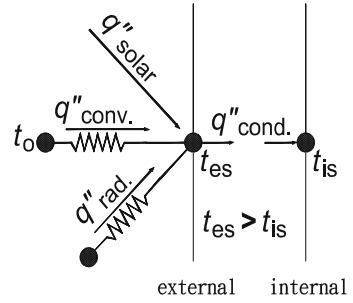
$q''_{\text{conduction}}$: Heat conduction flux ($\text{W}\cdot\text{m}^{-2}$)

q''_{solar} : Absorbed solar flux ($\text{W}\cdot\text{m}^{-2}$)

$q''_{\text{convection}}$: Heat convection flux ($\text{W}\cdot\text{m}^{-2}$)

$q''_{\text{radiation}}$: Radiation flux ($\text{W}\cdot\text{m}^{-2}$)

Fig. 2 Heat balance calculation Scheme



A. Absorbed solar flux q''_{solar} .

(a) *Opaque part calculated using Eq. (7):*

$$q''_{solar} = \epsilon(E_{t,b} + E_{t,d} + E_{t,r}) \tag{7}$$

(b) *Clear part:*

For part with no isolation coating using Eq. (8):

$$q''_{solar} = \epsilon_{1,b}^f E_{t,b} + \epsilon_{1,d}^f (E_{t,d} + E_{t,r}) \tag{8}$$

Without isolation coating using Eq. (9):

$$q''_{solar} = [\epsilon_{1,b}^f E_{t,b} + \epsilon_{1,d}^f (E_{t,d} + E_{t,r})] (1 - \epsilon_2^f) + E_{t,r} \epsilon_2^f \tag{9}$$

ϵ : Radiation absorptivity

$\epsilon_{1,b}^f$: Direct radiation absorptivity

$\epsilon_{1,d}^f$: Diffuse radiation absorptivity

ϵ_2^f : Isolation coating effect, 0.65 for absorption type, 0.35 for reflective type

B. External convection $q''_{convection}$ using Eq. (10):

$$q''_{convection} = h_o(t_o - t_{es}) \tag{10}$$

h_o : External convection coefficient ($W.m^{-2}.K^{-1}$)

t_o : External temperature (K)

C. The solar radiative heat gain $q''_{radiation}$ can be calculated using Eqs. (11, 12, 13, 14, 15, and 16):

$$q''_{\text{radiation}} = h_{r,g}(t_g - t_{es}) + h_{r,sky}(t_{sky} - t_{es}) \quad (11)$$

$$h_{r,g} = \varepsilon\sigma \left[\frac{F_{s-g}(t_g^4 - t_{es}^4)}{t_g - t_{es}} \right] \quad (12)$$

$$h_{r,sky} = \varepsilon\sigma \left[\frac{F_{s-sky}(t_{sky}^4 - t_{es}^4)}{t_{sky} - t_{es}} \right] \quad (13)$$

$$F_{s-g} = \frac{1 - \cos \alpha}{2} \quad (14)$$

$$F_{s-sky} = \frac{1 + \cos \alpha}{2} \quad (15)$$

$$t_{sky} = t_o - 6 \cos \frac{\alpha}{2} \quad (16)$$

$H_{r,g}$: Surface to ground radiation transfer coefficient ($\text{Wm}^{-2} \text{K}^{-1}$)

$H_{r,sky}$: Surface to sky radiation transfer coefficient ($\text{Wm}^{-2} \text{K}^{-1}$)

t_g : Ground surface temperature (K)

t_{sky} : Effective sky temperature (K)

ε : Surface long wave emissivity

σ : Stefan-Boltzmann constant, $5.67 \times 10^{-8} \text{W.m}^{-2}.\text{K}^{-4}$

F_{s-g} : Surface to ground view angle factor

F_{s-sky} : Surface to sky view angle factor

α : Surface inclination angle relative to the normal

t_{es} can be calculated by substituting Eqs. (7), (10) and (11) into (6) to obtain Eq. (17).

$$t_{es} = \frac{Ut_{set} + aG_t + h_o t_o + h_{r,g} t_g + h_{r,sky} t_{sky}}{U + h_o + h_{r,g} + h_{r,sky}} \quad (17)$$

Iteration is required in the computation as $h_{r,g}$, $h_{r,sky}$ and h_o (for natural convection) are determined based on the external surface temperature.

2.4 Outdoor Air-Cooling Load, Q_{Fresh}

Outdoor air ventilation is required to maintain the air quality inside an automobile. The outdoor air has to be treated to meet thermal comfort conditions. The cooling load due to fresh air ventilation can be calculated using Eq. (18).

$$Q_{\text{fresh}} = Q\rho_{\text{air}}n_p(h_{\text{out}} - h_{\text{in}}) \quad (18)$$

Q : Minimum air volume per person as given in ASHRAE standard 62.1 (2004) and can be set at $0.15 \text{ m}^3 \text{ min}^{-1} \text{ person}^{-1}$.

ρ_{air} : Air density, taken as 1.2 kg/m^3

N_p : Number of passengers

h : Air enthalpy (kJ.kg^{-1})

2.5 Heat Gain Due to Passengers, Equipment, and Lighting, Q_{inside}

$$Q_{\text{Inside}} = Q_{\text{human}} + Q_{\text{equ.}} + Q_{\text{light}} \quad (19)$$

Components of Eq. (19) are described below:

Q_{human} : $115 \text{ W} \times \text{number of person}$

$Q_{\text{equ.}}$: Include fan motor, GPS, stereo, electric equipment, estimated at 638 W

Q_{light} : Taken to zero at day time

3 Computation Software Development

Based on the cooling load computation model described above, an Excel-VBA based air-conditioning load calculation tool was developed. The cooling load calculation needs only conditions of ambient environment and the driving mode parameters such as speed and GPS information. With the highest temperature of the day known or predicted, the possible maximum load can be calculated. The design of automotive air conditioning and the control strategy can be performed with the calculation tool to save time and reduce costs. Prediction of the surface temperature of the shell structure can be calculated using the Excel-VBA based tool.

3.1 Experimental Measurements of Automobile Surface Temperature

A comparison of the prediction model with actual measurement of the outside shell temperature of a car was conducted. Figure 3 shows a sedan placed outside exposed to the sun. The comparison was made under the actual weather conditions such as temperature, humidity, and wind speed, car heading direction, sky clearness, and ground surface temperature.

Fig. 3 An automobile under test

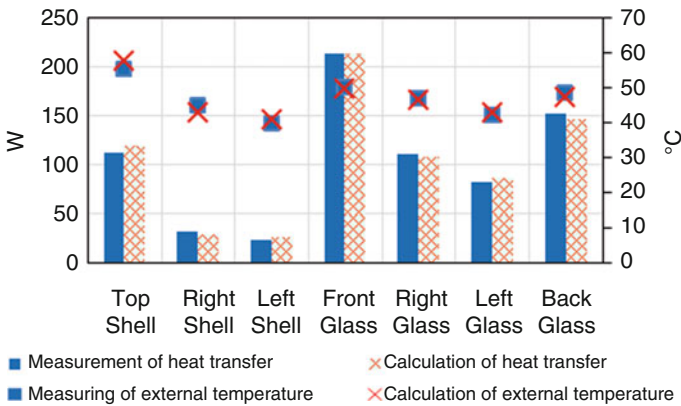


Fig. 4 Comparison of prediction and measurement of surface temperature and heat transfer

The measurements were carried out on a sunny day in 2013 at noon. Other measured data are described below:

1. Ground surface temperature was 60 °C.
2. Ambient air temperature was 32 °C.
3. Ambient air relative humidity was 49%.
4. Ambient air velocity was 1.3 m/s.

In the measurement, the automobile was headed towards south.

3.2 Verification of External Surface Temperature

The comparison between the prediction and the measurement of surface temperature and heat transfer are shown in Fig. 4. Comparison is made between the different glass and opaque areas. It can be seen that the errors for the opaque and glass areas are, respectively, ± 2.2 °C and ± 1 °C. The largest errors for temperature

and heat transfer are, respectively, 4.5% and $\pm 12\%$. The average errors for surface temperature and heat transfer are, respectively, 0.34% and 1.07%. As a whole the inner and outside car body temperatures were predicted to an accuracy of $\pm 1\text{ }^\circ\text{C}$.

4 Energy-Saving Potential Analysis

Energy saving has to first satisfy the thermal comfort of the passengers. However, energy saving is critical to the driving range. Air conditioning of electric vehicles is powered by the refrigerant compressor and the fans. This study focuses on the compressor power and the effects of driving modes and the ambient environment. Therefore the analysis presented in this paper reflects an energy saving potential that is closely related to the actual driving modes of electric vehicles.

4.1 Compressor Performance Curves

Figure 5 presents the performance curves of an electric vehicle refrigerant compressor as presented by Hsiao (2011). The compressor curves were used in the analysis of the compressor according to the needs of the air-conditioning capacity. It can be seen that the refrigerating capacity changes with the compressor speed, and compressor power changes with compressor speed. Note also the coefficient of performance (COP) for compressor peak at lower speed. COP peaks at about 4.6 at around 1300 rpm; however, at 3500 rpm COP reduces to about 1.5. Therefore it can

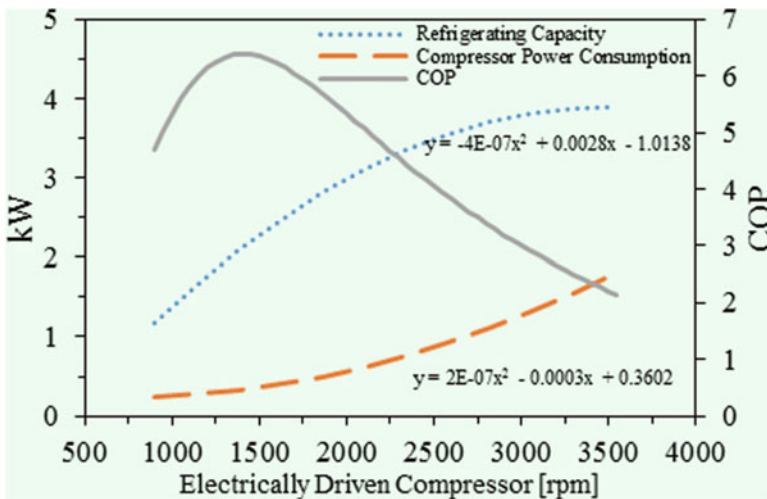


Fig. 5 The performance curves of a compressor

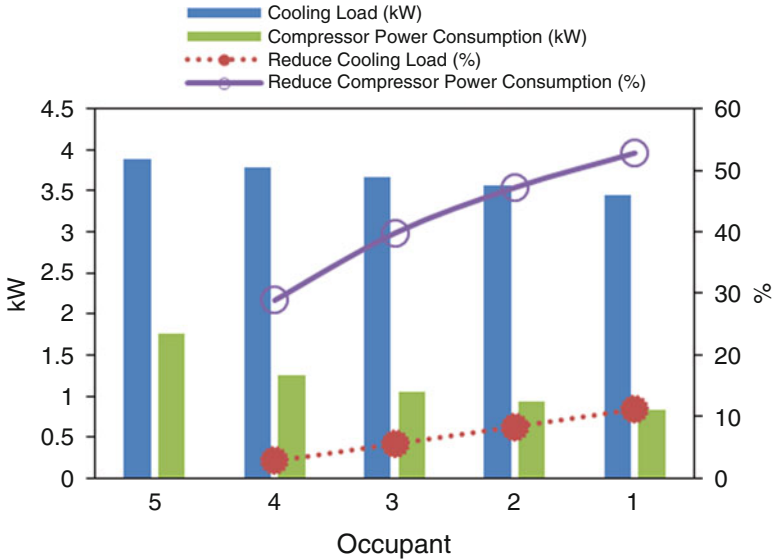


Fig. 6 Compressor energy saving for different numbers of passengers

be seen that the control strategy is key to energy saving for an air-conditioning system for electric vehicles. It is also obvious that the compressor must be kept at a lower speed whenever possible.

4.2 Control Strategy for Passenger Numbers

For vehicles with front and back seat air outlets, air-conditioning can be controlled to meet the actual need. When only the front seats are occupied, only front air outlets are turned on. Moreover, outdoor air supply volume can be controlled according to number of passengers in the car. Figure 6 shows the results of analysis. It can be seen that relative to five passengers, the cooling load can be reduced by about 11.2%. Also compressor power can be reduced by 28.9–52.8% when only one passenger is in the automobile. The high rate of energy saving is feasible, as discussed above, with compressor power being much lower at lower speed and at lower capacity.

4.3 Control Strategy to Meet the Driving Modes

In the course of a day a vehicle will be exposed to different temperature, humidity, and solar radiation conditions. Therefore the air-conditioning load will differ at

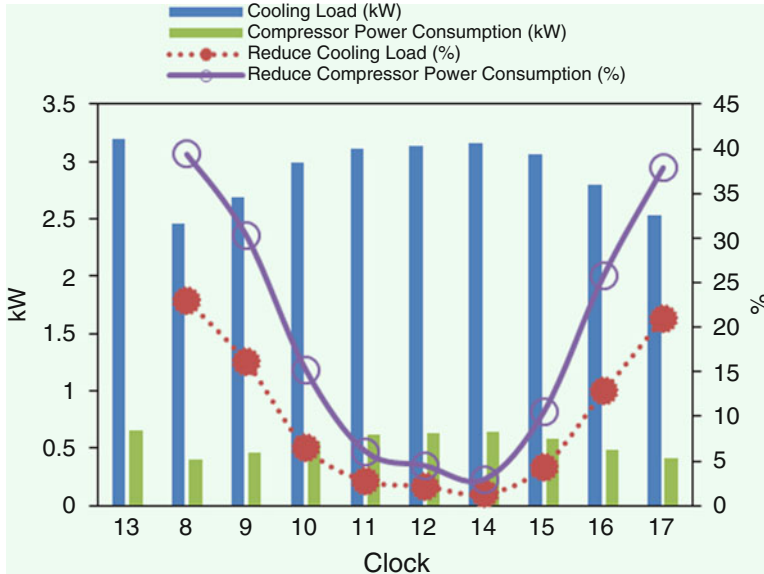


Fig. 7 Compressor power at different times of the day

different times. Figure 7 shows the analysis of the performance at different times of the day. Relative to the peak load that occurs at about 1:00 pm, the compressor power can be reduced by about 3–39% at other times when the compressor speed is controlled according to needs.

4.4 Control Strategy at Different Driving Speeds

The results of the analysis are shown in Fig. 8. It can be seen that cooling is highest when the vehicle is still at 0 km/h. This is due to a higher shell temperature when the car is not moving. A higher driving speed, however, was found to have a smaller cooling load. This is due to convective heat transfer that maintains the shell at a temperature approaching the ambient temperature. The cooling load reduces with speed up to 50 km/h, after that the effects of a lower cooling load are only marginal. It can be seen that the control strategy of compressor speed to meet the cooling load at different car speeds can reduce the compressor power by 44–62% with respect to a speed of 0.0 km/h.

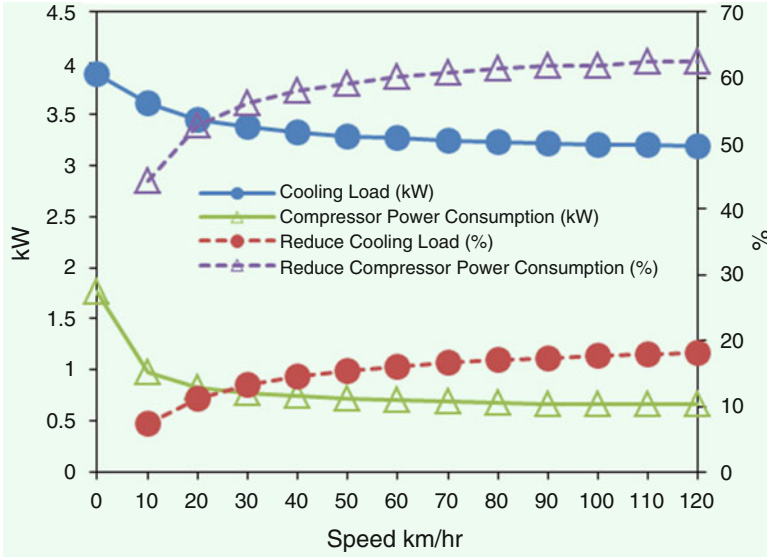


Fig. 8 Compressor at different speeds

4.5 Energy-Saving Analysis for a 1-h Drive

A small size black sedan with five passengers on board was simulated for a ride from 13:00 pm to 14:00 pm in the month of July and with clear skies. The results are shown in Fig. 9. The 1-h drive consists of 10 min of engine idling, 30 min at 30 km/h, and 20 min at 50 km/h. The solar effects were also modelled for each 10-min period. The vehicle was assumed to drive south with an outdoor air temperature and humidity of 33.9 °C and 58% RH, respectively. The temperature and humidity inside the car were set at 23 °C and 55% RH, respectively.

The results of the analysis are also presented in Table 1. It can be seen that for the 1-h driving schedule mentioned above, when the compressor can be controlled to adapt to the air-conditioning needs, energy can be saved by as much as 50.4%.

5 Discussion on Energy Management Adapted to Driving Modes

Energy saving measures for air conditioning are very important for electric- or hybrid-powered vehicles. The driving range of a charged battery can be affected greatly by the air-conditioning needs. In particular, it is necessary to allow air-conditioning control to adapt to different driving modes under different ambient conditions.

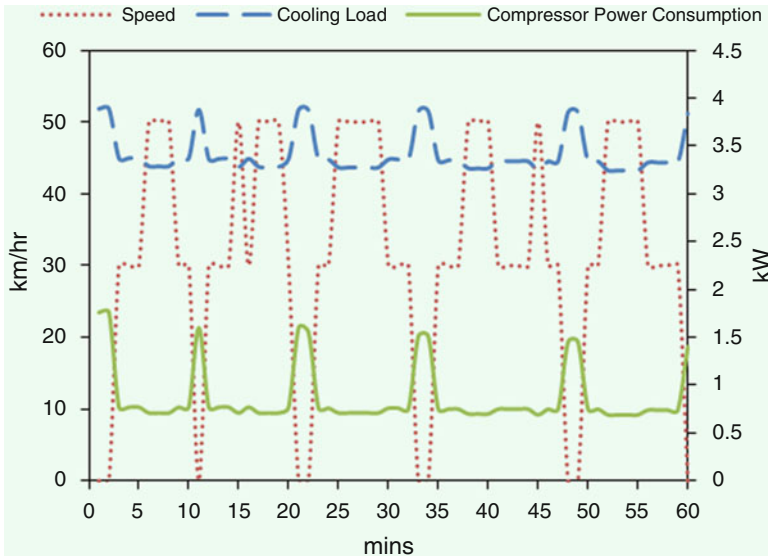


Fig. 9 Analysis of cooling load and compressor power for a 1-h drive

Table 1 Air-conditioning energy analysis for 1 h of driving

Item	Operate at highest load	Control to the cooling need
Driving time (min)	60	60
Cooling need (W)	3887	3243 ~ 3887
Compressor power (kW)	1.76	0.69 ~ 1.76
Energy used (kWh)	1.76	0.87
Energy saving rate relative to operating at highest load (%)	–	50.4

A DC variable speed compressor, electronic expansion valve, and other controls can be used to regulate the power use of automotive air conditioning. The occupants’ comfort can be satisfied by multi-air outlets for different seating in a vehicle. It has been shown that compressor power is strongly dependent on compressor speed. Further optimization of the compressor operation matching the cooling capacity could be a control strategy in future research.

6 Conclusion

A cooling-load computation model is proposed in this paper. A comparison of the prediction with the actual measurement has shown the car body's temperatures were predicted to an accuracy of ± 1 °C. Optimization of the compressor operation matching the cooling capacity can save compressor power by as much as 52.8%. It was also found that a lighter color car has a lower cooling load. At higher driving speeds convective heat transfer would maintain the car shell at temperatures approaching the ambient temperature and result in lower energy being used. A single drive consists of different driving modes, and when adapting to the air-conditioning needs, energy-saving control can reduce the energy use by 50.4%.

Acknowledgment The support of the National Science Council of Taiwan with project NSC 101-2221-E-027 -047 is gratefully acknowledged.

References

- Alkan, A., Hosoz, M.: Comparative performance of an automotive air-conditioning system using fixed and variable capacity compressors. *Int. J. Refrig.* **33**, 487–495 (2010)
- ANSI/ASHRAE Standard 62.1-2004. Ventilation for Acceptable Indoor Air Quality. ASHRAE, Atlanta, USA (2004)
- ASHRAE Handbook, Fundamentals, Chapter 4. ASHRAE, Atlanta, USA (2009a)
- ASHRAE Handbook, Fundamentals, Chapter 14. ASHRAE, Atlanta, USA (2009b)
- Brown, J.: New low global warming potential refrigerants. *ASHRAE J.* 22–29 (2009)
- Hosoz, M., Direk, M.: Performance evaluation of an integrated automotive air conditioning and heat pump system. *Energy Convers. Manag.* **47**, 545–559 (2006)
- Hsiao, P.: A study on refrigerant volume control and energy parameters for electric powered vehicle air-conditioning systems. Master Thesis, National Taipei University of Technology (2011)
- IEA. <http://iea.org/newsroomandevents/news/2013/february/name,35176,en.html>
- Lee, Y., Jung, D.: A brief performance comparison of R1234yf and R134a in a bench tester for automobile applications. *Appl. Therm. Eng.* **35**, 240–242 (2012)
- Makino, M., Ogawa, N., Abe, Y., Fujiwara, Y.: Automotive air-conditioning electrically driven compressor, SAE technical paper series 2003-01-0734 (2003)
- Nakane, S., Kadoi, M., Seto, H., Prigain, K.: Air-conditioning system for electric vehicle. *JSAE.* **64**(4), 35–40 (2010)